Strong Piezoelectricity in Bioinspired Peptide Nanotubes

Andrei Kholkin,[†,*] Nadav Amdursky,[‡] Igor Bdikin,[§] Ehud Gazit,[‡] and Gil Rosenman[∥,*]

[†]Department of Ceramics and Glass Engineering & CICECO, University of Aveiro, 3810-193 Aveiro, Portugal, [‡]Department of Molecular Microbiology and Biotechnology, George S. Wise Faculty of Life Sciences, Tel Aviv University, Tel Aviv 69978, Israel, [§]Centre for Mechanical Technology & Automation, University of Aveiro, 3810-193 Aveiro, Portugal, and [∥]School of Electrical Engineering, Iby and Aladar Fleischman Faculty of Engineering, Tel Aviv University, Tel Aviv 69978, Israel

ABSTRACT We show anomalously strong shear piezoelectric activity in self-assembled diphenylalanine peptide nanotubes (PNTs), indicating electric polarization directed along the tube axis. Comparison with well-known piezoelectric $LiNbO_3$ and lateral signal calibration yields sufficiently high effective piezoelectric coefficient values of at least 60 pm/V (shear response for tubes of $\approx$200 nm in diameter). PNTs demonstrate linear deformation without irreversible degradation in a broad range of driving voltages. The results open up a wide avenue for developing new generations of "green" piezoelectric materials and piezonanodevices based on bioactive tubular nanostructures potentially compatible with human tissue.

P iezoelectricity is the ability of non-centrosymmetric crystals to produce mechanical stress/strain under electric field or charge under mechanical stress. This property has long been used in acoustic transducers, sensors/actuators, piezomotors, and more.[1] Pushed by the technology progress, superior energy density, and low energy consumption, piezoelectrics have recently experienced a drastic miniaturization giving rise to a new direction commonly abbreviated as piezoMEMS (for MicroElectroMechanical Systems).[2,3] Recent success in developing piezoelectric nanotubes has shown their great potential.[4] Unfortunately, the best piezoelectric studied over the last 50 years, $Pb(Zr,T)O_3$ (PZT), has to be sintered at high temperature (at least 600 °C) and is sensitive to stoichiometry, defects, and microstructure, making it difficult to scaling down and integrating with IC technology.[3] Nonferroelectric piezoelectrics such as ZnO have been proposed for the use in piezoMEMS.[5] Most inorganic piezoelectrics are intrinsically incompatible with biological environment and can be even harmful. Hence, organic[6] and bio-organic materials having significant piezoactivity are indispensible to revolutionize

the piezoMEMS. However, as for today, only weak piezoelectric effects in bio-organic materials have been observed (see ref. 7 for a recent review). Therefore, the search for micro- and nanoscale piezoelectric materials has drawn much attention in the last decades.[2−5]

Several natural biomaterials (plants, animals, human tissues) studied both by classical methods[8,9] and nanoscale techniques[10,11] were found to possess weak piezoelectricity. To the best of our knowledge (see, *e.g.*, refs 7, 10, and 11 and references therein), the highest piezocoefficient in biomaterials measured so far is $\sim$20 pm/V[12] (scleral collagen); however, it is unstable due to dehydration. Therefore, the search for bioinspired materials exhibiting strong and robust piezoelectricity is a task of utmost importance. Another challenge is to fabricate the nanostructural material such as nanotubes for the activation of piezoelectricity at the nanoscale.[5]

In the present study, we report our finding of piezoactivity in bioactive peptide nanotubes (PNT) made by a self-assembly process of small diphenylalanine, $NH_2-Phe-Phe-COOH$ (FF), peptide monomers. These PNTs have first been discovered from the determination of the smallest recognition motif of the amyloid-β protein, the protein of Alzheimers disease.[13] They are made from biological building blocks—amino acids, thus having intrinsic biocompatibility and other unique properties such as high Young modulus.[14] X-ray and electron diffraction have revealed that their crystal structure is compatible with a space group $P6_1$ (noncentrosymmetric),[15] which allows for many physical phenomena described by the odd-rank tensor (*e.g.*, piezoelectricity and pyroelectricity).[16,17] In

*Address correspondence to kholkin@ua.pt; gilr@eng.tau.ac.il.

this work, we were able to examine the piezoelectric activity of PNTs owing to the recent progress in scanning probe techniques.[18,19]

RESULTS AND DISCUSSION

Figure 1a shows a representative AFM image of the PNTs assembled on a Au/Si substrate. A variety of tubes of different lengths, diameters, and orientations were observed. Following the topography acquisition, the AFM was switched to the piezoresponse force microscopy (PFM) regime in which the conducting tip is scanned in contact mode while an ac voltage (V_{ac}) is applied between the tip and Au electrode (Figure 1b). In these conditions, we could measure both out-of-plane (OOP) and in-plane (IP) polarization components.[20] When the scan is performed along the tube axis, we were able to detect IP signal due to a shear component of the piezotensor (d_{15}), corresponding to the polarization parallel to the tube axis, and OOP that reflects polarization along the tube radius (Figure 1b). The fact that we observed only the shear component (Figure 1c,d and 3) unequivocally suggests that the only polarization component existing in PNTs is along the tube axis.

Piezoelectric OOP signal as evidenced by Figure 2e,f was close to zero. Two types of piezoelectric profiles were observed in PNTs, irrespectively of their external diameter, R. The bell-shape profile (Figure 2a,c) is attested to tubes with high outer to inner (r) diameter ratios (R/r) where the internal cavity does not significantly affect the E-field distribution and resulting piezosignal (i.e., penetration depth of the E-field is comparable or smaller than the wall thickness). To avoid the influence of any geometrical constraints on the cantilever torsion and IP signal detection, we always used the maximum contrast value for the analysis (arrow on Figure 1d). In some cases, we observed a two-hump profile (Figure 2b,d) where the piezosignal dropped to about half of its maximum value. This situation reflects the distortion of the applied E-field due to the presence of the cavity. These results are in line with recent PNT profiling obtained using electrostatic force microscopy.[21] In the following, we restrict ourselves to only presenting the results of single-hump nanotubes in which piezoresponse can be readily analyzed as a function of PNT position, R, and V_{ac}.

In order to understand the origin of piezoresponse, we should consider the possible d_{ij} matrix for the space group $P6_1$.[17] In this group, only two shear components exist, which apparently describe deformations along two perpendicular axes relative to the tube axis. In the configuration shown in Figure 1b, the component of the shear deformation is parallel to the tube axis and proportional to $1/2 d_{15} V_{ac} \cos \alpha$, where α is the angle between the tube axis and scanning direction and d_{15} is the shear piezocoefficient. In order to prove the piezo-

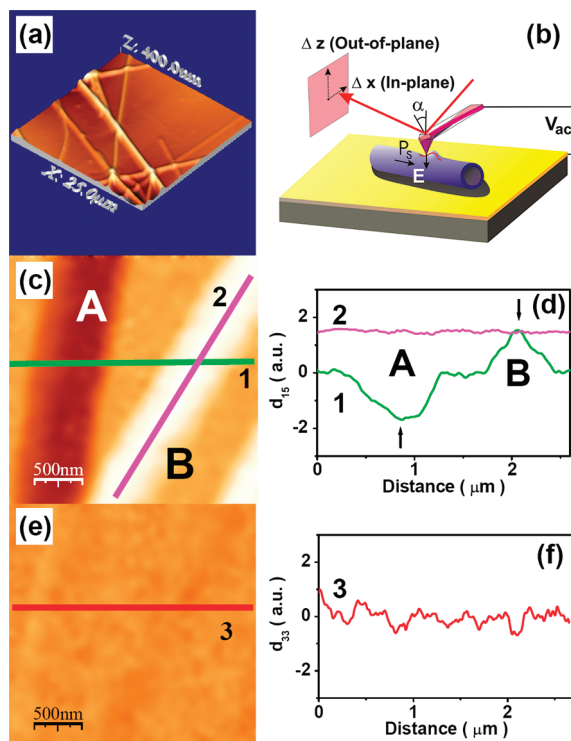**Figure 1. (a)** Topography of as-deposited PNTs on Au-coated substrate (scan 25 × 25 μm²), **(b)** schematic of the nanoscale in-plane measurements by PFM, **(c)** IP piezoresponse of two tubes (A and B) with oppositely directed polarizations, **(d)** cross sections of the IPP image across (1) and along (2) the tube axis, demonstrating different sign and uniformity of polarization, **(e)** OOP image of the same tubes, and **(d)** cross section of (e) along line 1. V_{ac} = 2.5 V, f = 5 kHz.

electric nature of the contrast, data on all tubes having the same diameter (≈100 nm) were analyzed as a function of α (Figure 3). The data are in perfect agreement with the expected cosine function (Figure 3d). The con-

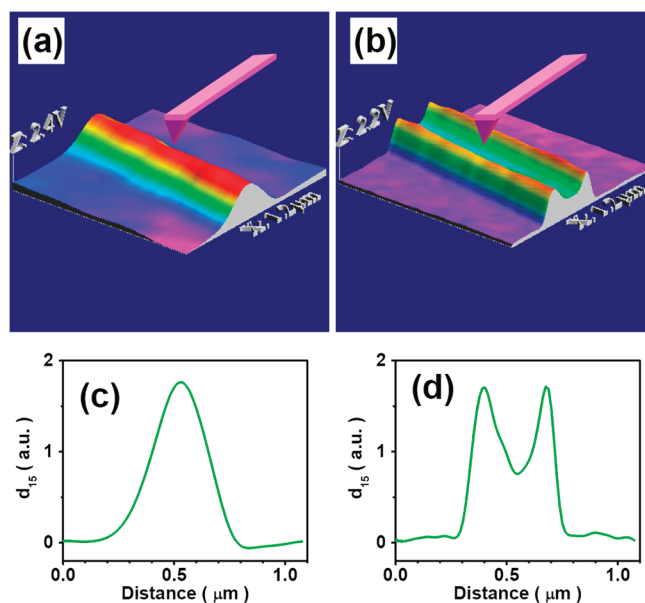**Figure 2.** In-plane piezoresponse images of single PNTs for large **(a)** and small **(b)** R/r ratios. **(c,d)** Cross sections of (a) and (b), respectively. V_{ac} = 2.5 V, f = 5 kHz.
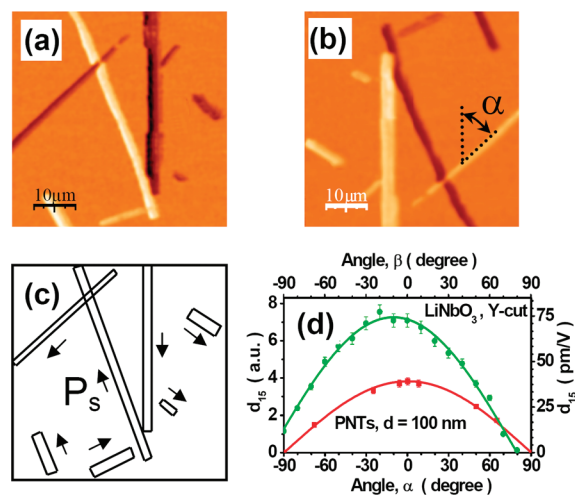
Figure 3. IP PFM images of peptide nanotubes before (a) and after (b) rotation at 180° (V_{ac} = 2.5 V, f = 5 kHz) demonstrating apparent contrast reversal. (c) Schematic of the tube polarizations deduced from PFM images. (d) IP signal—angle dependences for representative tube (α) and Y-cut LiNbO$_3$ (β) reference sample made under the same conditions. The labels on the right ordinate axis represent the absolute values of the effective shear piezoelectric coefficients calculated based on the bulk values of LiNbO$_3$.[27]

trast is completely reversed when the sample was physically rotated at 180° (*cf*. Figure 3a,b). Both features have contrast reversal and a predicted $d_{15}(\alpha)$ dependence point to the piezoelectric origin of the signal. This also rules out possible contribution of spurious electrostatic signal as it suggests only OOP component.[19] In addition, piezoresponse signal was independent of the vertical force (Supporting Information, Figure S1), and force—distance curves for PNTs were identical to those taken on a rigid substrate (Supporting Information, Figure S2) without any sign of mechanical indentation of the former. This excludes possible artifacts related to electric-field-controlled stiffness and slip motion of the tip.

Since the PFM gives only the effective piezoresponse, that is, the volume average of the surface vibrations caused by the inhomogeneous E-field distribution,[22] it is worth comparing the results with a well-known piezoelectric such as LiNbO$_3$ (LNO). In this way, the piezoeffect in PNTs can be roughly quantified without rigorous calculations[23] that are complicated because of the tubular geometry. Figure 3d demonstrates
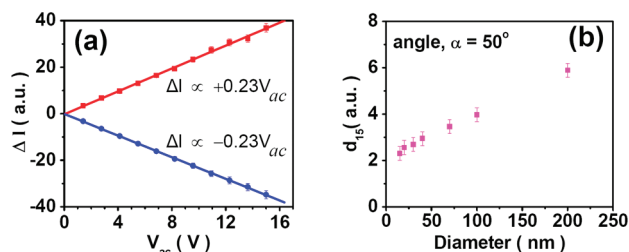

Figure 4. (a) Ac voltage dependences of IP displacements Δ*I* for tubes with opposite polarization directions (*R* ~ 200 nm). (b) Representative dependence of the shear piezoresponse as a function of the tube external diameter *R*. V_{ac} = 2.5 V, f = 5 kHz.

similar angle dependence measured under identical conditions on the Y-cut surface of LNO crystals with 3*m* symmetry. If the cantilever is scanned parallel to the *Z*-direction of the Y-cut LNO, there is only one component of the shear displacement that is present when the E-field is applied along the *Y*-direction.[24]

For the arbitrary orientation of the crystal, the same equation, $1/(d_{15}V_{ac}\cos\beta)$, applies, where now β is the angle between the scanning direction and the *Z*-axis. As shown in Figure 3d, we observed the same dependence with the maximum value slightly shifted to the negative side. The observed maximum excludes any angle dependence (critical for shear response) and allows direct comparison of the piezoelectric activities in both materials. It is seen that the effective d_{15} coefficient for a 100 nm tube is about 2 times smaller than in bulk LNO,[25,26] thus giving the value of ≈35 pm/V. Taking into account almost linear dependence of the piezocontrast on *R*, we can claim that in tubes with $R \gtrsim 200$ nm the deformation is roughly the same as in classical piezoelectric LiNbO$_3$.[26,27] These values were confirmed by using the lateral signal calibration as described in the recent work on piezoelectric collagen fibrils.[28] In short, we calculated lateral sensitivity of the Si cantilever based on the calibrated vertical sensitivity and the dimensions of the used conducting probe. The lateral sensitivity was about 2 mV/nm, and the values of the displacements divided by the applied voltage could serve also as a rough measure of piezoactivity in PNTs. These values were about 50% greater than those calculated based on the comparison with table values of LNO[26,27] and thus confirmed once again that shear deformations in PNTs are remarkably strong, comparable to LNO crystals and much greater than in collagen fibrils.[28]

The piezoelectric anisotropy (*i.e.*, the ratio between d_{15} and d_{33}) is unknown for PNTs, but for a vast majority of ferroelectric materials, it varies between 1.3 (PZT)[29] and 10−12 (LNO).[26] It means that the expected value for the longitudinal piezocoefficient for PNTs (not accessible by our measurements) is between ≈5−6 (as for LNO) and ≈50 pm/V (as for PZT). In order to further prove the piezoelectric nature of the signal, we measured the ac voltage dependences of deformation for two oppositely oriented tubes (Figure 4a). As expected, two straight lines were observed without any nonlinearity or irreversibility even at a high ac voltage of 16 V (see also Figure S3 of Supporting Information). It signifies that the observed piezoresponse is very stable and PNTs can be driven under high excitation level. There was no visible degradation (within the measurement accuracy) of the topography after driving during prolonged time (tens of minutes). Another striking feature is the observed dependence of the piezoresponse on the tube diameter (Figure 4b). It is natural to assume that, for sufficiently thick walls, the piezoresponse (shown on Figure 3a) will depend only on the piezoproperties of the PNT material underneath, rather than on the geometrical constraints. If the inner diameter

of the tube r is constant (irrespectively of the outer diameter R), the observed dependence on R can be qualitatively explained by the transition from "thin" to "thick" wall case where piezoelectric properties should approach to "bulk" piezoelectric effect in the latter. This scenario is consistent with the existence of two piezoelectric profiles (Figure 3a,b) and probably describes a transition between two extreme cases. Finite element modeling studies of the tubes could be indispensable to understand and quantify the apparent size effect, but the calculations require knowledge of the geometrical parameters (i.e., inner diameter of the tubes) and elastic/piezoelectric coefficients currently unavailable in the literature.

CONCLUSIONS

We have found a fundamental physical effect—piezoelectricity in bio-organic nanostructures made from peptide building blocks. The strong and robust piezoelectric activity in bioinspired PNTs (never seen in the past) makes them promising candidates for future generations of "green" nanopiezoelectrics that might be extensively used in biomedical and medical applications. It is foreseen that these biocompatible and rigid nanotubes (as well as arrays of thereof) may serve as the key elements for future biosensors allowing direct contact with human tissue.

MATERIALS AND METHODS

PNTs were prepared by dissolving the FF building blocks in lyophilized form in 1,1,1,3,3,3-hexafluoro-2-propanol at a concentration of 100 mg/mL. The stock solution was diluted to a final concentration of 2 mg/mL in ddH_2O for the nanotube self-assembly process to occur. The diluted solution was dried onto a gold-coated silicon surface (150 nm Au, 15 nm Cr). The measurements were done with a commercial AFM (Ntegra Prima, NT-MDT) equipped with external function generator and lock-in amplifier (see more details in ref 19). We used doped Si cantilevers with spring constants in the range of 0.02−1 N/m driven at a frequency of 5 kHz.

Supporting Information Available: Figure S1 demonstrates independence of the measured piezoresponse on static force up to 110 nN. Data on Figure S2 compares force−distance curves made on PNTs and on hard mica substrate. Figure S3 illustrates full reversibility of the piezoelectric response under high driving voltage (up to 16 V). This material is available free of charge via the Internet at http://pubs.acs.org.

REFERENCES AND NOTES

1. *Piezoelectric and Acoustic Materials for Transducer Applications*; Safari, A., Akdogan, E. K., Eds.; Springer: Boston, MA, 2008.
2. Polla, D. L.; Francis, L. F. Ferroelectric Thin Films in Micromechanical Systems Applications. *MRS Bull.* **1996**, *21*, 59–65.
3. Muralt, P. Recent Progress in Materials Issues for Piezoelectric MEMS. *J. Am. Ceram. Soc.* **2008**, *91*, 1385–1396.
4. Morrison, F. D.; Luo, Y.; Szafraniak, I.; Nagarajan, V.; Wehrspohn, R. B.; Steinhart, M.; Wendroff, J. H.; Zakharov, N. D.; Mishina, E. D.; Vorotilov, K. A.; *et al.* Ferroelectric Nanotubes. *Rev. Adv. Mater. Sci.* **2003**, *4*, 114–122.
5. Wang, Z. L. The New Field of Nanopiezotronics. *Mater. Today* **2007**, *10*, 20–28.
6. Horiuchi, S.; Tokura, Y. Organic Ferroelectrics. *Nat. Mater.* **2008**, *7*, 357–366.
7. Gruverman, A.; Rodriguez B. J.; Kalinin, S. V. Electromechanical Behaviour in Biological Systems at the Nanoscale. In *Scanning Probe Microscopy: Electrical and Electromechanical Phenomena at the Nanoscale*; Kalinin, S., Gruverman, A., Eds.; Springer: Berlin, 2006; Vol. 1, pp 615−633.
8. Shamos, M. H.; Lavine, L. Piezoelectricity as a Fundamental Property of Biological Tissues. *Nature* **1967**, *213*, 267–269.
9. Fukada, E.; Yasuda, I. On the Piezoelectric Effect of Bone. *J. Phys. Soc. Jpn.* **1957**, *12*, 1158–1162.
10. Halperin, C.; Mutchnik, S.; Agronin, A.; Molotskii, M.; Urenski, P.; Salai, M.; Rosenman, G. Piezoelectric Effect in Human Bones Studied in Nanometer Scale. *Nano Lett.* **2004**, *4*, 1253–1256.
11. Rodriguez, B. J.; Kalinin, S. V.; Shin, J.; Jesse, S.; Grichko, V.; Thundat, T.; Baddorf, A. P.; Gruverman, A. Electromechanical Imaging of Biomaterials by Scanning Probe Microscopy. *J. Struct. Biol.* **2006**, *153*, 151–159.
12. Ghosh, S.; Mei, B. Z.; Lubkin, V.; Scheinbeim, J. I.; Newman, B. A.; Kramer, P.; Bennett, G.; Feit, N. Piezoelectric Response of Scleral Collagen. *J. Biomed. Mater. Res.* **1998**, *39*, 453–457.
13. Reches, M.; Gazit, E. Casting Metal Nanowires within Discrete Self-Assembled Peptide Nanotubes. *Science* **2003**, *300*, 625–627.
14. Kol, N.; Adler-Abramovich, L.; Barlam, D.; Shneck, R. Z.; Gazit, E.; Rousso, I. Self-Assembled Peptide Nanotubes Are Uniquely Rigid Bioinspired Supramolecular Structures. *Nano Lett.* **2005**, *5*, 1343–1346.
15. Gorbitz, C. H. Nanotube Formation by Hydrophobic Dipeptides. *Chem.—Eur. J.* **2001**, *7*, 5153–5159.
16. Haussuhl, S. Electro-Optic, Dielectric, Elastic and Thermoelastic Properties of Hexagonal Cs_2S_2O6, $LiClO_4 \cdot 3H_2O$, $LiClO_4 \cdot 3D_2O$, and $Ba(NO_2)_2 \cdot H_2O$. *Acta Crystallogr., Sect. A* **1978**, *34*, 547–550.
17. Liminga, R.; Abrahams, S. C.; Bernstein, J. L. Absolute Sense and Model for the Piezoelectric and Pyroelectric Coefficients in $Ba(NO_2)_2 \cdot H_2O$ and $Cs_2S_2O_6$. *J. Appl. Crystallogr.* **1980**, *13*, 516–520.
18. *Nanoscale Characterization of Ferroelectric Materials*; Alexe, M., Gruverman, A., Eds.; Springer Verlag: Berlin-Heidelberg, 2004.
19. Kholkin, A. L.; Kalinin, S. V.; Roelofs, A.; Gruverman, A. Review of Ferroelectric Domain Imaging by Piezoresponse Force Microscopy. In *Scanning Probe Microscopy: Electrical and Electromechanical Phenomena at the Nanoscale*; Kalinin, S., Gruverman, A., Eds.; Springer: New York, 2006; Vol. 1, pp 173−214.
20. Abplanalp, M.; Eng, L. M.; Günter, P. Mapping the Domain Distribution at Ferroelectric Surfaces by Scanning Force Microscopy. *Appl. Phys. A: Mater. Sci. Process.* **1998**, *66*, S231–S234.
21. Clausen, C. H.; Jensen, J.; Castillo, J.; Dimaki, M.; Svendsen, W. E. Qualitative Mapping of Structurally Different Dipeptide Nanotubes. *Nano Lett.* **2008**, *8*, 3692–3695.
22. Kalinin, S. V.; Rar, A.; Jesse, S. A Decade of Piezoresponse Force Microscopy: Progress, Challenges, and Opportunities. *IEEE Trans. Ultrason. Ferroelectr. Freq. Control* **2008**, *53*, 2226–2252.
23. Eliseev, E. A.; Kalinin, S. V.; Jesse, S. Electromechanical Detection in Scanning Probe Microscopy: Tip Models and Materials Contrast. *J. Appl. Phys.* **2007**, *102*, 014109-12.

24. Heider, U.; Weis, O. Distortion-Free, Calibrated LiNbO$_3$ Piezoscanner for Probe Microscopies with Atomic Resolution. *Rev. Sci. Instrum.* **1993**, *64*, 3534–3537.

25. Warner, A. W.; Onoe, M.; Coquin, G. A. Determination of Elastic and Piezoelectric Constants for Crystals in Class 3*m*. *J. Acoust. Soc. Amer.* **1967**, *42*, 1223–1231.

26. Smith, T. R.; Welsch, F. S. Temperature Dependence of the Elastic, Piezoelectric, and Dielectric Constants of Lithium Tantalate and Lithium Niobate. *J. Appl. Phys.* **1971**, *42*, 2219–2230.

27. Landolt, H.; Bornstein R. *Numerical Data and Functional Relationships in Science and Technology, New Series, vol. III/16*; Springer Verlag: Berlin, 1981.

28. Minary-Jolandan, M.; Yu, M. F. Uncovering Nanoscale Electromechanical Heterogeneity in the Subfibrillar Structure of Collagen Fibrils Responsible for Piezoelectricity of Bone. *ACS Nano* **2009**, *3*, 1859–1863.

29. Jaffe B.; Cook W. R.; Jaffe H. *Piezoelectric Ceramics*; Academic Press: New York, 1971.